International Journal of Automotive Technology
https://doi.org/10.1007/s12239-024-00147-y

ELECTRIC, FUEL CELL, AND HYBRID VEHICLE, FUELS AND LUBRICANTS, HEAT TRANSFER, FLUID AND THERMAL ENGINEERING, VISION AND SENSORS

Prediction Models of Overall Thermal Sensation and Comfort in Vehicle Cabin Based on Field Experiments

Xin Xu[1,2] · Lanping Zhao[2,3] · Zhigang Yang[1,2]

Received: 27 June 2024 / Revised: 5 August 2024 / Accepted: 16 August 2024

Abstract
Vehicle thermal comfort has received more attention due to advancements in autonomous driving and intelligent cabin technology. Prediction of thermal comfort is challenging due to the passenger compartment's complex transient non-uniform thermal environment. Many thermal comfort models are primarily based on environmental or human thermal physiology factors, but too many temperature measurements may affect driving behavior. This study analyzed the correlations between local thermal sensation (LTS), local thermal comfort (LTC), the thermal environment in an automobile's cabin, and skin temperature. The optimal combination of influencing factors was established in the prediction model of overall thermal sensation (OTS) and overall thermal comfort (OTC) in the vehicle cabin. The results indicated that breathing air and chest skin surface temperature had the best correlation with subjective human evaluation. The prediction models of OTS and OTC have good prediction performance, and their R^2 values are 0.77 and 0.51, respectively. Accurately predicting the thermal comfort in the vehicle provides a valuable reference for intelligent cabin thermal environment control and automobile energy savings.

Keywords Vehicle thermal comfort · Local thermal sensation · Overall thermal sensation · Local thermal comfort · Overall thermal comfort

1 Introduction

People are paying more attention to vehicle thermal comfort as autonomous driving and intelligent cabin develop and improve. The driver's physiology, psychology, and driving safety are all impacted by thermal comfort. Researchers are trying to find a way to strike a balance between energy efficiency and thermal comfort (Croitoru et al., 2015; Nastase et al., 2022). However, due to the vehicle's highly transient and non-uniform thermal environment, no accepted model can accurately and conveniently forecast the vehicle thermal comfort.

Air velocity, air temperature, humidity, and average radiant temperature are environmental elements that affect human thermal comfort. Personal factors that affect thermal comfort include human activity level and clothing thermal resistance (Danca et al., 2016; Neacsu et al., 2017). Extensive experimental study on human thermal sensation and comfort in vehicle passenger compartments has been carried out, which can be divided into climate chamber experiments and field experiments according to the testing place. The advantage of climate chambers is that the environment can be controlled to avoid the impact of external environmental change on human thermal comfort inside the vehicle.

Some studies investigated the relationship between local and global thermal sensations and skin temperature by creating different in-vehicle thermal environments with air supply conditions in a controlled external environment (Lee et al., 2020). Relative humidity influences human thermal comfort in the passenger compartment of an automobile to a certain extent, and the results of some studies have shown

✉ Lanping Zhao
lanpingzhao@tongji.edu.cn

[1] School of Automotive Studies, Tongji University, Shanghai 201804, China

[2] Shanghai Key Lab of Vehicle Aerodynamics and Vehicle Thermal Management Systems, Shanghai 201804, China

[3] Institute of Refrigeration and Cryogenic Engineering, School of Mechanical Engineering, Tongji University, Shanghai 201804, China

that controlling the relative humidity can make the driver and passenger reach the thermal comfort state more quickly (Alahmer et al., 2012; Hepokoski et al., 2018, 2021). Heat conduction plays an important role in the exchange of heat between humans and the thermal environment inside the vehicle. In winter conditions, seat heating can rapidly improve human thermal comfort during the initial warming phase (Hu et al., 2024; Oi et al., 2011, 2012). There are apparent differences between field and climate chamber experiments. The field experiments under parking and driving conditions were conducted, combined with human thermal physiological, and psychological factors, and analyzed the correlation between environmental and human parameters and subjective evaluation (Xu et al., 2022). Except for human thermal comfort, vehicle cabin cooling energy consumption and air quality satisfaction are also analyzed (Kaynakli et al., 2004, 2005; Kilic et al., 2010, 2012). Yun et al. (2021) conducted field tests on 80 female subjects and obtained an overall thermal sensation prediction model based on environmental parameters. In addition, some studies have studied the differences between parking and driving conditions (Mao et al., 2018; Zhou et al., 2019). The results showed significant differences in drivers' thermal comfort, sensitivity, and preference under driving conditions. The thermal acceptability of the driver is better than that of the parking condition due to the driver's concentration. Recently, Kim et al. (2023) conducted a study on the correlation between multiple physiological parameters and in-vehicle thermal comfort, and their findings suggest that long-term use of HVAC heating modes reduces drivers' thermal comfort and concentration. In winter driving, physiological changes in drivers preceded environmental changes and drivers' psychological responses were faster than physiological responses under different heating modes.

Thermal comfort is the result of people and their thermal environment under the action of thermal regulation. In the past decades, researchers have researched the thermal comfort model. Fanger (1967) proposed the famous PMV-PPD model based on the human thermal balance theory, and its application background was a steady and uniform thermal environment. Wyon et al. (1989) proposed the notion of equivalent homogeneous temperature (EHT) obtained by skin temperature and heat flow. Then, the thermal comfort interval of each part of the human body was divided by subjective evaluation related to thermal comfort. The EHT evaluation index is applicable to the steady-state non-uniform thermal environment, but cannot make an evaluation of the whole body. Zhang et al., (2009, 2013) studied the connection between subjective evaluation and environmental and human parameters through environmental chamber experiments. The models of local and overall thermal sensation and thermal comfort are proposed. The Berkeley model can predict human thermal comfort in a transient non-uniform thermal environment. The results showed that the thermal comfort obtained in a transient non-uniform thermal environment might be higher than that felt in a neutral and uniform thermal environment.

Up to now, the previous thermal comfort models established by scholars have been based on environmental factors or human factors. Few prediction models of thermal comfort in an automobile cabin consider environmental and human factors. In addition, the existing non-uniform thermal comfort model needs to measure a large amount of information to figure up vehicle thermal sensation and comfort, which is difficult to measure in authentic passenger cabins and affects driving behavior. The thermal comfort in the vehicle passenger compartment was examined in this study, and the relationships between thermal sensation and comfort, the interior surface and air temperature, and skin temperature were measured and analyzed. Finally, based on environmental and human factors, prediction models for vehicle overall thermal sensation and overall thermal comfort were developed.

2 Materials and Methods

2.1 Experimental Conditions

The thermal comfort experiments of the human body in vehicle cabins were conducted while parked in both summer (July) and winter (January) in Shanghai, China. The experimental vehicle is a compact sedan with four-gear air conditioning. All experiments were carried out under variable air supply speeds with constant heat exchange. Table 1 shows the ambient temperature and air supply conditions for all summer and winter experiments, where tests 1–16 are for summer conditions and tests 17–32 are for winter conditions. The average environmental temperature of summer and winter experiments were 35.3 and 9.5 ℃, respectively. The average supply air temperature decreased with the decrease of supply air speed in summer experiments and increased in winter experiments. The air supply speed and temperature refer to the average of the four air conditioning outlets. During the investigation, the air conditioner maintained the blowing surface mode of internal circulation. We measured the intensity of solar radiation during the summer experiments. While the winter experiments were mostly conducted at night, so the effect of solar radiation was neglected.

2.2 Experiment Contents and Instruments

The interior surface and air temperature are required to be measured because the thermal environment plays an important role in the thermal comfort of the vehicle cabin. Figure 1 (a) depicts the experiment's interior surface and air temperature measurement points. The interior surface

Table 1 Environment temperature and air supply conditions

	Test1	Test2	Test3	Test4	Test 5	Test 6	Test 7	Test 8	Test 9	Test10
Average air supply temperature (℃)	13.9	12.6	7.6	8.0	13.5	9.7	7.5	7.3	12.8	9.4
Average air supply speed (m/s)	7.7	5.1	3.8	2.4	7.7	5.1	3.8	2.4	7.7	5.1
Average environment temperature (℃)	36.2	34.6	34.7	34.6	34.9	36.0	36.2	35.3	35.0	36.0
	Test11	Test12	Test13	Test14	Test15	Test16	Test17	Test18	Test19	Test20
Average air supply temperature (℃)	6.8	7.0	14.5	10.6	6.8	7.7	37.5	48.6	58.9	66.7
Average air supply speed (m/s)	3.8	2.4	7.7	5.1	3.8	2.4	7.7	5.1	3.8	2.4
Average environment temperature (℃)	34.9	34.3	31.3	32.2	31.8	31.7	8.7	12.2	10.5	11.6
	Test21	Test22	Test23	Test24	Test25	Test26	Test27	Test28	Test29	Test30
Average air supply temperature (℃)	35.0	45.9	59.6	67.2	36.1	52.1	61.3	66.5	43.8	46.4
Average air supply speed (m/s)	7.7	5.1	3.8	2.4	7.7	5.1	3.8	2.4	7.7	5.1
Average environment temperature (℃)	13.4	14.1	11.7	14.6	7.3	7.2	6.9	6.8	6.7	6.7
	Test31	Test32								
Average air supply temperature (℃)	55.7	66.9								
Average air supply speed (m/s)	3.8	2.4								
Average environment temperature (℃)	6.5	6.3								

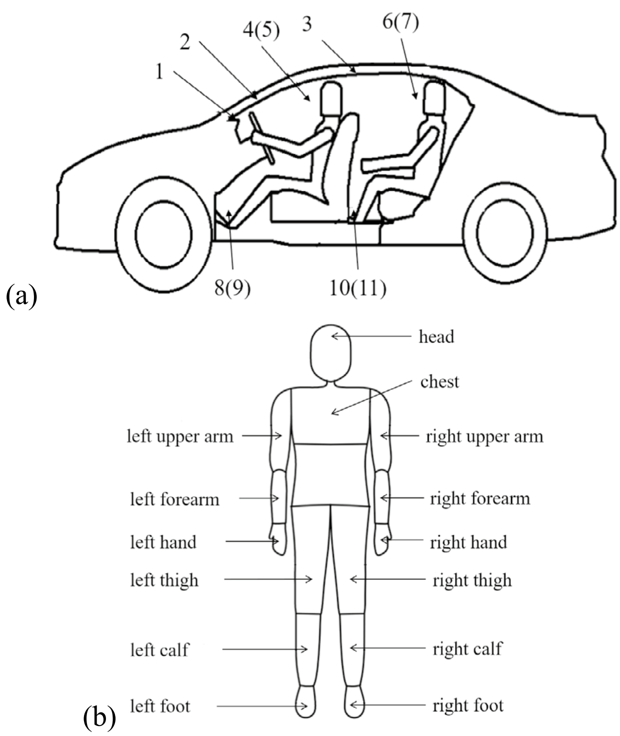

Fig. 1 Measuring point location:**a** for cabin interior surface and air temperature and **b** for skin temperature of experimental subjects

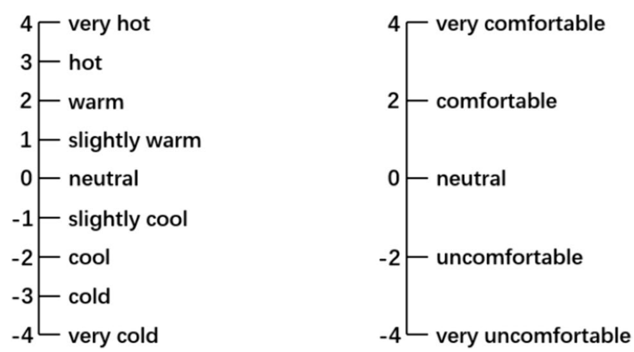

Fig. 2 Scales of thermal sensation and thermal comfort

measurement points include the dashboard (#1), windshield (#2), and roof (#3). Air temperature measurement points also include air supply vents, foot (#8-#11) and breathing point air (#4-#7) temperature at all four seats, and outside ambient air. The result of thermal regulation in the thermal environment of the vehicle cabin is partially reflected in the skin temperature. The human body parts measured in the experiment are shown in Fig. 1(b). Medical adhesive tape was used to secure the thermocouple in the center of each body part. The mean skin temperature was calculated using the seven-point method proposed by Hardy and Dubois [35] as shown in Eq. (1). Where MST is the mean skin temperature, T is the skin temperature of each site, and the weights of each site are shown in Equation. The scales used in the questionnaire to rate subjective thermal sensation and thermal comfort are shown in Fig. 2.

Two different types of Omega thermocouples were used for the experimental measurements. The wire diameter of the TT-K-24-SLE thermocouple is thicker than the TT-K-36-SLE. In order to gauge the temperature of environmental factors, we used TT- K-24-SLE thermocouples.

Additionally, the TT-K-36-SLE thermocouple was employed to measure the temperature of the human skin surface. The measuring range of the thermocouple is—200 ~ 260 °C, and its uncertainty is ± 0.5 °C. The data logger is Keysight 34972A, and the airspeed in the vehicle passenger compartment was measured by Fluke 925 hand-held impeller anemometer, which measuring range is 0.4 ~ 25 m/s and uncertainty is ± 2%.

$$\begin{aligned} MST = {} & 0.07 * \left(T_{Head}\right) + 0.35 * \left(T_{Chest}\right) \\ & + 0.14 * \left(T_{LowerArm}\right) + 0.07 * \left(T_{Foot}\right) \\ & + 0.13 * \left(T_{LowerLeg}\right) + 0.19 * \left(T_{Thigh}\right) \\ & + 0.05 * \left(T_{Hand}\right) \end{aligned} \tag{1}$$

Fig. 3 Experimental scene diagram

2.3 Subjects

Thirty-two healthy graduate students (26 males and six females), aged between 20 and 24, participated in the experiment. Males' average height and weight are 173.2 cm and 66.5 kg, respectively. And females' average height and weight are 164.7 cm and 50 kg, respectively. Before the experiment, the purpose and procedure of the experiment were informed. In addition, the subjects were required to rest sufficiently and not drink alcohol, smoke, or exercise vigorously before the experiment. Regarding clothing thermal resistance, all subjects were required to put on short-sleeved t-shirts, shorts, and slippers when participating in experimental summer conditions. The clothing requirements for subjects in winter experiments were hoodies and jeans.

2.4 Experiment Procedure

Before the experiment, we checked the air conditioning performance of the experimental automobile and arranged the thermocouple at the specified position of the temperature measurement point. The subjects changed into experimental clothing in the preparation room and reached thermal equilibrium in a uniform thermal environment. The subjects were given another explanation of the experiment's goal and methodology at the same time by the researchers. The researchers assisted the subjects to secure thermocouples and measured their skin surface temperature as soon as they entered the passenger compartment and turned on the vehicle air conditioning to simulate the test environment. The experimental data were recorded when the thermal environment of the cabin was stabilized. When the interior surface, air, and human skin temperature were stabilized after the experiment ran for 30 min, the subjects were instructed to complete the subjective evaluation questionnaire. The next air supply condition experiment was then performed. After the atmosphere was stabilized, each experiment lasted 30 min, and data were taken every 10 s by the data gathering device. The experimental scene diagram is depicted in Fig. 3.

2.5 Fitting Function for the Prediction Model

The experimental data were compiled to examine the connection between human thermal sensation and comfort, skin temperature and the thermal environment in the vehicle's passenger compartment. We found that vehicle cabins' human thermal sensation and comfort vary significantly among experimental personnel, even with the same thermal environment. The thermal sensation increases with increasing skin temperature and thermal environment. And with the increase of thermal sensation or skin surface temperature, thermal comfort first increases and then decreases. According to the various characteristics of thermal sensation and thermal comfort, suitable functions were selected for fitting analysis, respectively.

A logistic function fits the human thermal sensation to the experimental and human factors. Equation (2) is the logistic function used in this paper, where A value reflects the slope of thermal sensation altering with the temperature of the environment and skin surface. The value of B represents the neutral skin temperature of the study body part. It exhibits the characteristics shown in Fig. 4, with the linearity in the middle leveling off as the skin temperature increases or decreases. A Gauss function fits the human thermal comfort to the environment's temperature, skin surface, and thermal sensation. The Gauss function is presented in Eq. (3). The value of y0 + A reflects the height of the curve spike, w equals the standard variance,

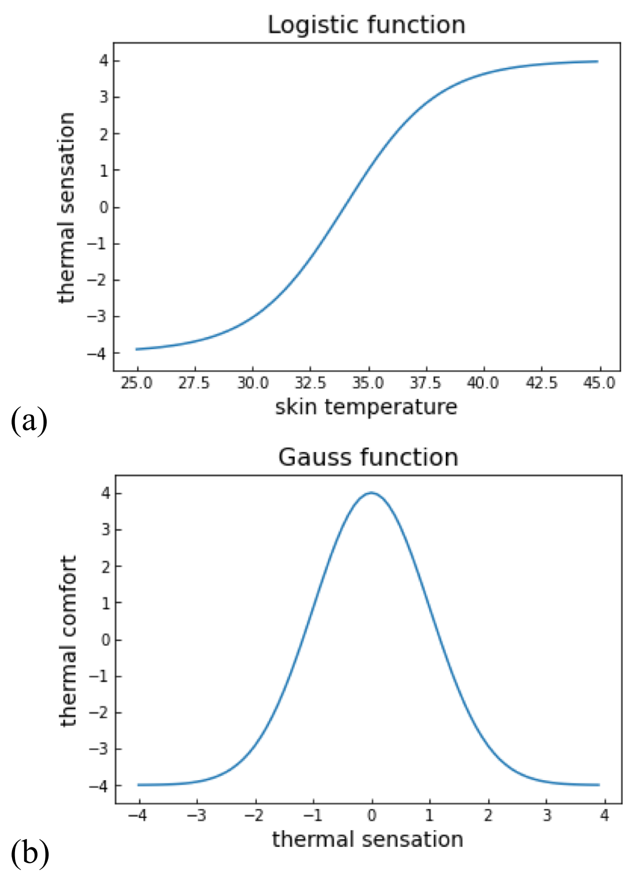

Fig. 4 Logistic function and gauss function

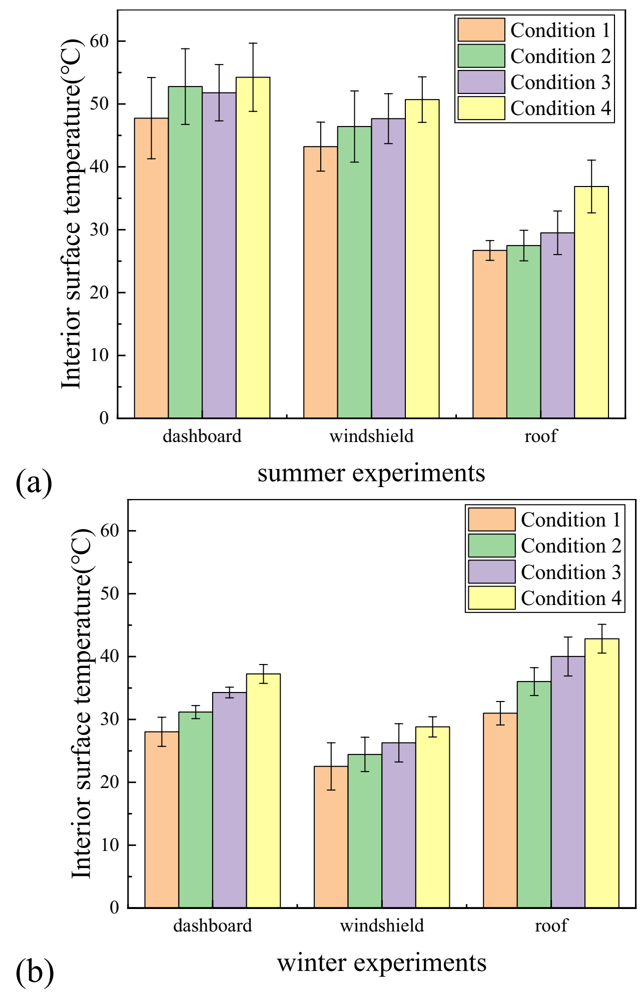

Fig. 5 Interior surface temperature

and xc represents the coordinates of the spike center. Human thermal comfort increases first and then decreases with the increase in skin temperature and thermal sensation. The function image has a single peak value, indicating that thermal comfort reaches the optimal value at a specific skin temperature or thermal sensation.

$$y = \frac{8}{(1 + \exp(-A * (x - B)))} - 4 \tag{2}$$

$$y = y0 + Ae^{-\frac{(x-xc)^2}{2w^2}} \tag{3}$$

3 Results

3.1 Thermal Environment in the Vehicle Passenger Compartment

Temperature is the most commonly used physical quantity to characterize the thermal environment and human thermal physiology. Existing research has established several human thermal comfort models in the laboratory environment, but the research on vehicle thermal comfort based on field experiments is relatively few. Through this study, we hope to get the relationship between objective physical quantity and human subjective evaluation. The exact quantities selected in this study included temperature of typical interior surfaces, vehicle cabin air, ambient and skin surface. We analyzed all tests categorized by wind speed, with four conditions.

As proven in Fig. 5, the temperature of three distinct surfaces in the vehicle's passenger compartment: the dashboard, the windshield, and the roof. Condition 1–4 represent four different experimental conditions of supply air speeds from high to low. In summer experiments, the dashboard is the hottest of the three interior surfaces, followed by the windshield and roof. In the winter experiment, the surface temperature inside the cabin were the roof, dash and windshield in descending order. As a result of the effect of solar radiation in summer, the average temperature of the dashboard in condition 4 is 54.2 °C even if the air conditioner is on, and the average windshield is 50.7 °C. The reason is that the solar radiation acted on the dashboard through the windshield. And the glass is less absorbent, making the dashboard hotter than the windshield. The interior roof is not directly influenced by solar radiation and has the lowest temperature of 36.9 °C under the influence of air conditioning. However, the solar radiation intensity is weak in winter, and its effect on the interior surface is less than that of air conditioning. The roof is the surface most affected by air conditioning in these three surfaces, and its temperature is the highest in the winter experiments. The average temperature of the roof in condition 4 is 42.8 °C, which is higher than that in all summer experiments. And the dashboard temperature is 37.2 °C. The windshield is the lowest of the three interior surfaces, 28.8 °C.

Cabin air temperature, including those around the feet and heads of the driver, co-driver, and rear passenger, are shown in Fig. 6. Even under steady-state conditions, the air temperature in the passenger compartment of a vehicle exhibits extreme heterogeneity both horizontally and vertically. In general, the degree of non-uniformity in the vehicle passenger compartment in winter experiment conditions is higher than in summer, and the vertical temperature difference is larger than the horizontal temperature difference. In terms of vertical air temperature difference, the air temperature around the feet was higher than the air temperature around the head under summer experimental conditions. The opposite was true in winter conditions. The cause is that in the air conditioning face-blowing mode, the effect of air conditioning on the air around the head is more significant than that of the feet. The vertical temperature difference in the vehicle cabin is more critical in winter experiments than in summer experiments because the supply air and the ambient temperature difference is much more significant in winter experiments than in summer experiments. Under the summer experiments, the average vertical temperature difference is 0.8 °C. At the same time, the value in winter is much higher than in summer (8.6 °C), and the vertical temperature difference increases as the air supply speed decreases. The vertical air temperature difference in winter test 4 is as high as

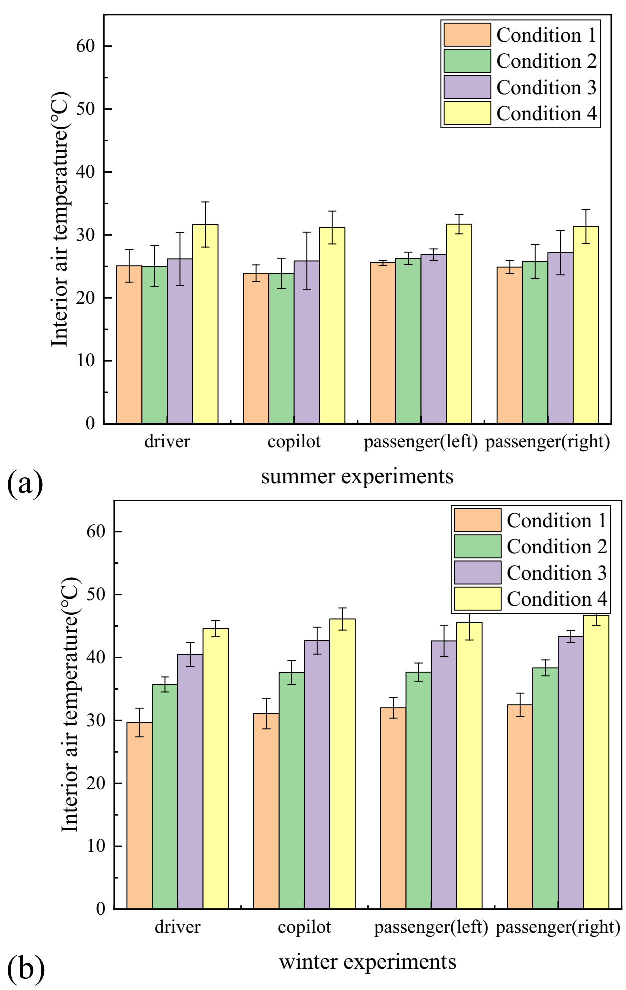

Fig. 6 Interior air temperature. **a, b** Breathing air, **c, d** foot air

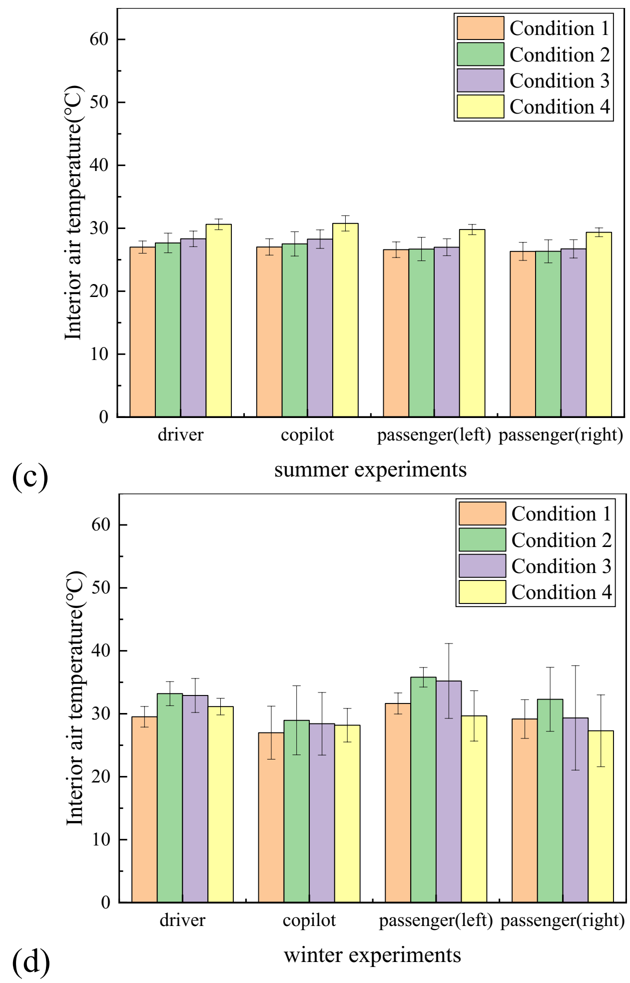

Fig. 6 (continued)

16.7 °C. As for the horizontal air temperature difference, it is mainly affected by the uneven air supply and thermal boundary conditions. The temperature difference of breathing air is smaller than that of the air underfoot, and the temperature difference between the front driver and passenger is larger than that between the rear passengers.

3.2 The Influence of Air Supply Conditions

Figure 7 depicts the mean skin temperature, overall thermal sensation, and thermal comfort of the subjects under different air supply conditions. It can be observed from the figure that the mean skin temperature of the subjects increased in both summer and winter experiments as the airspeed decreased. The results of the summer experiments align with common sense, while the winter experiments demonstrate this phenomenon due to our experimental design involving a variable air velocity under constant heat exchange. Consequently, the temperature of the air supply rises as the air velocity decreases. Within the existing experimental conditions, the impact of air supply temperature on skin temperature is more significant than that of air supply speed. Furthermore, there is a notable positive correlation between thermal sensation and mean skin temperature, while thermal comfort experiences a decline in both summer and winter conditions when the airspeed decreases.

3.3 The Relationships Between Solar Radiation and Overall Thermal Perception

In addition to air supply conditions, solar radiation intensity has a greater effect on in-vehicle thermal comfort in summer conditions, so the correlation between solar radiation and in-vehicle human thermal comfort was analyzed. In Fig. 8, we performed a linear fit between solar radiation intensity and the overall thermal perception of the human body inside the car and found that under the summer tests in this study, the overall thermal sensation of the subjects inside the car increased with the increase of solar radiation intensity, and the opposite is true for the overall thermal comfort, for every increase of solar radiation intensity by 100 W/m2, the overall thermal sensation increased by 1.6, and the overall thermal comfort decreased by 1.4. In addition, we can see a good correlation between the overall thermal sensation of the subjects inside the car under the steady-state conditions and that of the subjects inside the car under the summer working conditions, so we analyzed the correlation between solar radiation and human thermal comfort. In addition, we can see that the correlation between solar radiation and the overall thermal sensation in steady-state condition is good, with an R^2 value of 0.83. However, the correlation between thermal comfort and solar radiation intensity is poorer, with an R^2 value of 0.33. The reason for this is that thermal

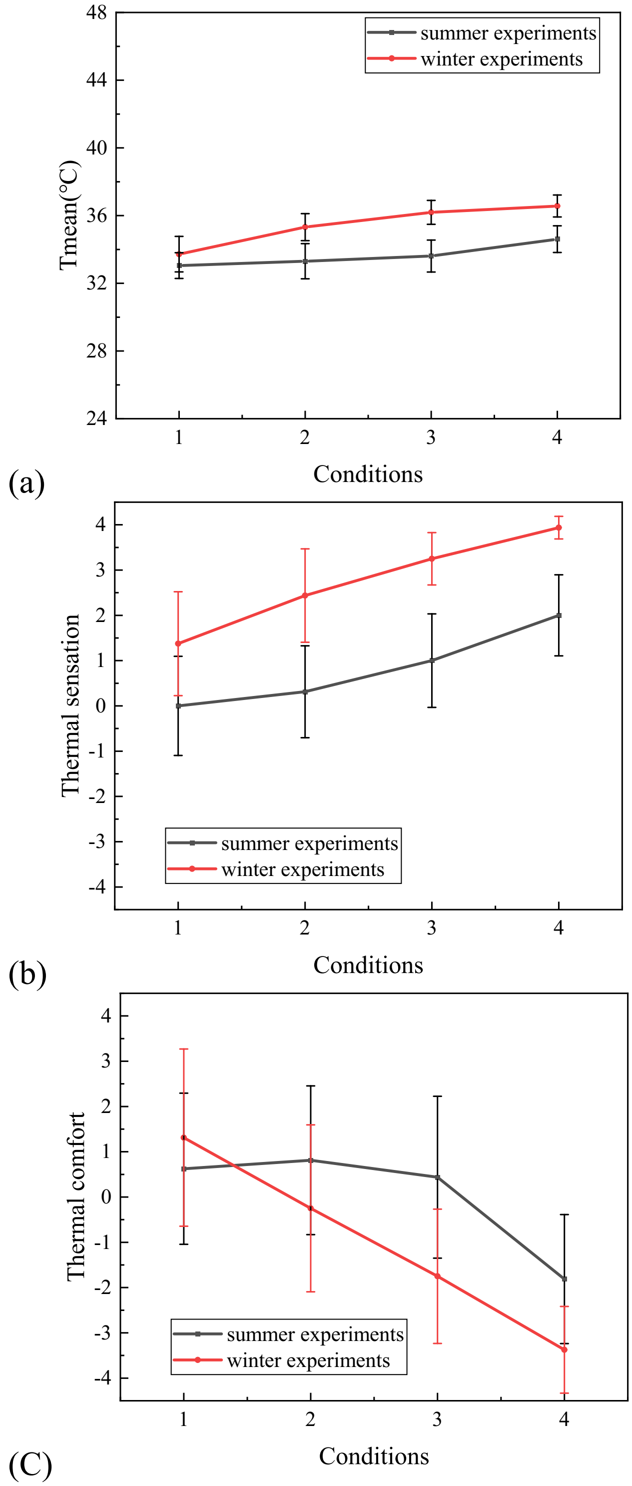

Fig. 7 The influence of air supply conditions. **a** Mean skin temperature, **b** thermal sensation, **c** thermal comfort

comfort is more affected by the subjective influence, and the difference is more significant between different subjects.

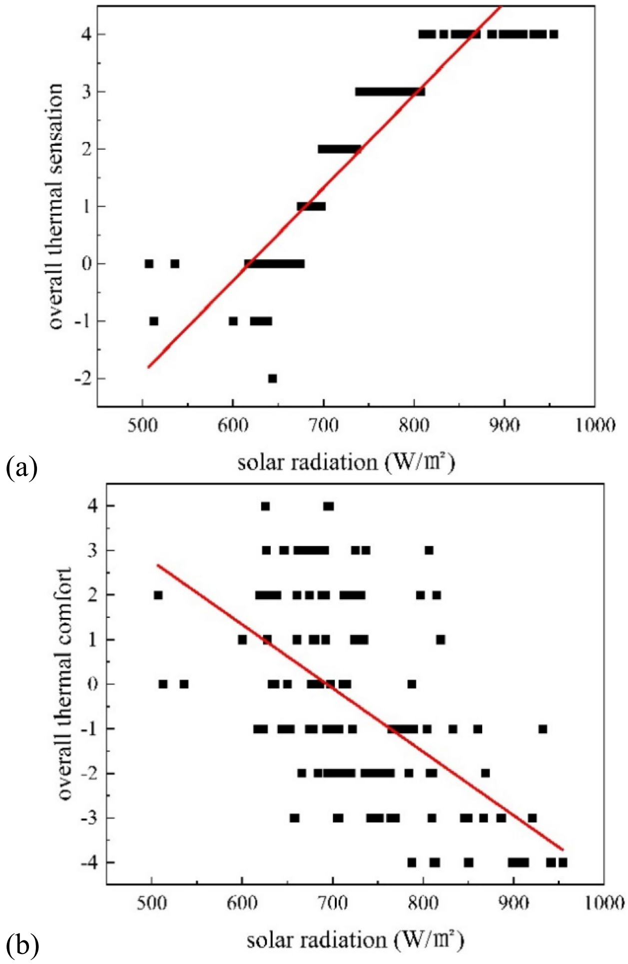

Fig. 8 Relationship between solar radiation and overall thermal sensation and thermal comfort

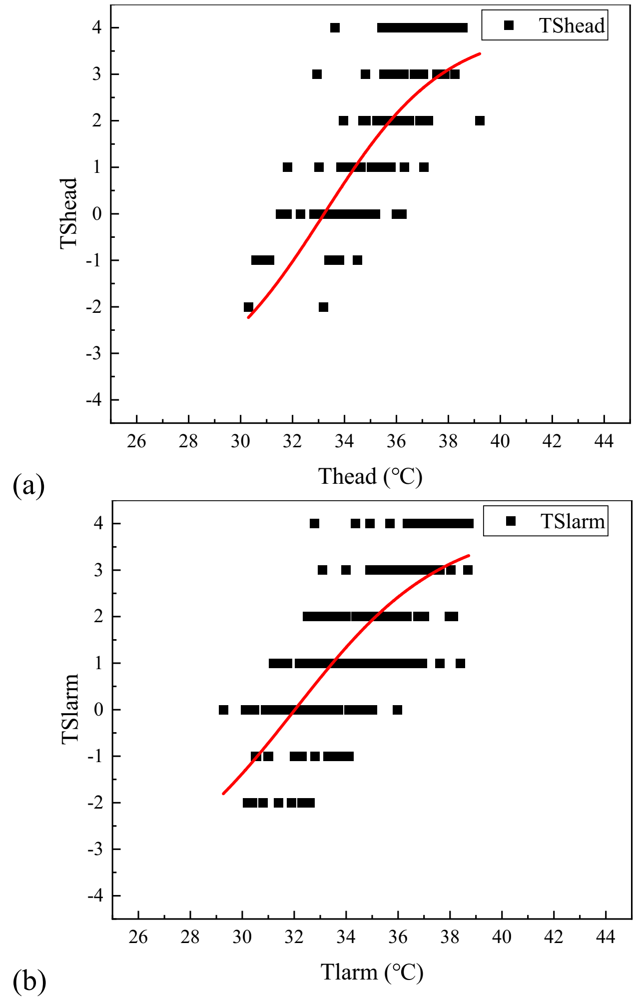

Fig. 9 Correlation between local thermal sensation (LTS) and local skin temperature (LST)

3.4 Local Thermal Sensation and Local Thermal Comfort

Figure 9 shows the connection between the head and lower arm's local skin temperature (LST) and the local thermal sensation (LTS). With an A value of 0.52 and a slope of the thermal trend with skin temperature that is greater than the limbs, the chest has the greatest slope of all body parts. The neutral temperature of the head and chest are similar and higher than that of the other extremities. Among all local body parts, the coefficient of determination of lower arm skin temperature and thermal sensation is the greatest, where the R^2 value is around 0.6.

Figure 10 analyzes the relationship between local thermal comfort (LTC), local skin temperature (LST), and local thermal sensation (LTS). Table 2 gives the R^2 and local thermal sensation of local thermal comfort with respect to local skin temperature. The chest had the highest correlation among all body parts. The R^2 value of the nonlinear regression of local skin temperature with local thermal comfort is 0.5, and the R^2 value of local thermal sensation with local thermal comfort is 0.48. The correlation between local skin temperature and local thermal comfort is more uncertain than the correlation between local skin temperature and thermal sensation. It was found that predicting local thermal comfort by local thermal sensation could obtain better R^2 values than predicting local thermal comfort by local skin temperature (Fig. 11).

3.5 Overall Thermal Sensation and Overall Thermal Comfort

It is obvious that the overall thermal sensation and overall thermal comfort are more meaningful for evaluating the vehicle's thermal environment. As a result, the correlation between the vehicle thermal environment, the interior surface, the local skin surface, the mean skin surface, and the

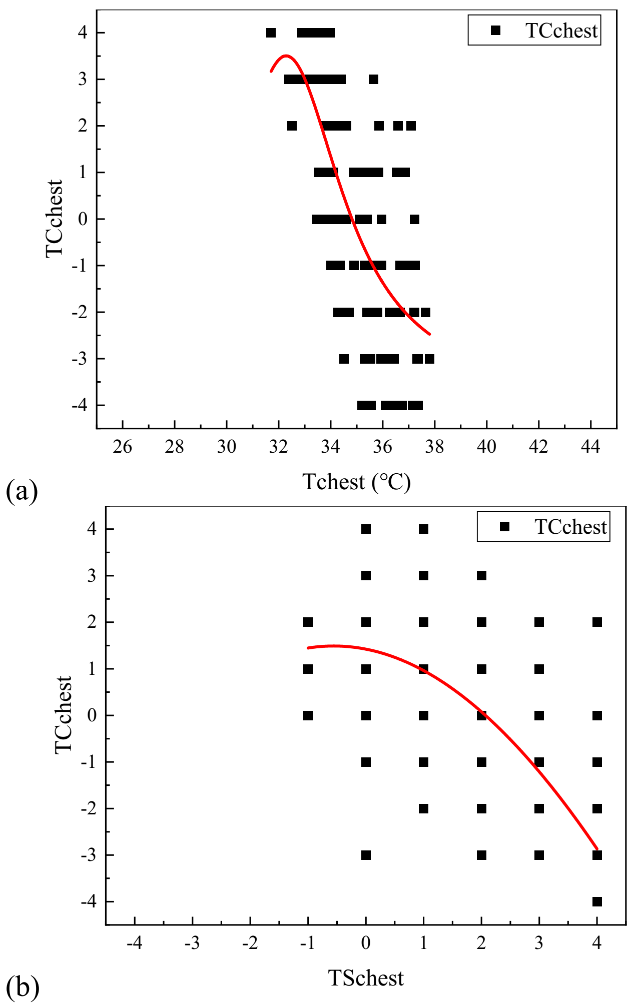

Fig. 10 Correlation between local skin temperature (LST), local thermal sensation (LTS) and local thermal comfort (LTC)

overall thermal sensation and comfort were analyzed. First, the influences of thermal environment parameters, including the air temperature inside and outside the vehicle and interior surface, on the overall thermal sensation and thermal comfort were analyzed. The logistic function was used to fit and analyze the correlation between thermal environmental factors, overall thermal sensation, and overall thermal comfort. The R^2 value of the influence of respiration temperature on the overall thermal sensation of the human body is up to 0.58, indicating its essential impact on the overall thermal sensation of the human body in the passenger compartment.

The correlation between overall thermal comfort and thermal environment is lower than that between overall thermal sensation and thermal environment. Among the six environmental parameters, breathing air temperature correlated more significantly than other environmental parameters (Table 3).

In addition, the air and interior surface temperature reflect the thermal environment inside the vehicle. In contrast, skin temperature reflects the occupant's thermal physiological state, and the two factors together can better describe the differences in human thermal comfort. A logistic function was used to fit each local body and average skin temperature to the overall thermal sensation. The data in the table show that the overall thermal sensation correlates more with the average skin temperature than with the skin temperature of each local area. Among all body parts, the fitting R^2 value of chest skin temperature and the overall thermal sensation was the closest to the mean skin temperature, followed by the head, whose R^2 values were 0.54 and 0.46, respectively. The Gaussian functions were used to fit the correlation between skin temperature and overall thermal comfort. Local skin temperature on the hands and calves were significantly correlated with overall thermal comfort with R^2 values of 0.43 and 0.44, respectively (Fig. 12, Table 4).

The linear fitting method analyzed the local and overall thermal sensation and comfort. Figure 13 shows the chest's regression lines; the X-axis is the local subjective evaluation of the chest, and the Y-axis is the overall personal evaluation. Table 5 gives the correlation between thermal sensation and thermal comfort of each body part and the whole-body. It is found that the chest is relatively correlated with the whole body. All other bodily locations' thermal comfort and sensation have correlation coefficients that are less than 0.5. Additionally, the limbs' correlation coefficients for thermal comfort are lower than their correlation coefficients for thermal sensation. The findings showed that there is a stronger association between local thermal sensitivity in these body parts and overall thermal sensation than there is between local thermal comfort in these body areas and overall thermal comfort.

3.6 Regression Analyses and Models

Through the results obtained in Sect. 3.5, we selected the breathing air temperature as the thermal environment factor and the chest skin temperature as the human body factor.

Table 2 R^2 between local skin temperature (LST), local thermal sensation (LTS) and local thermal comfort (LTC)

Body part	Head	Chest	Upper arm	Lower arm	hand	Thigh	Calf	Foot
R^2 (LST and LTS)	0.54	0.49	0.50	0.60	0.39	0.29	0.44	0.36
R^2 (LST and LTC)	0.33	0.50	0.38	0.39	0.30	0.29	0.36	0.28
R^2 (LTS and LTC)	0.48	0.48	0.38	0.43	0.43	0.37	0.30	0.31

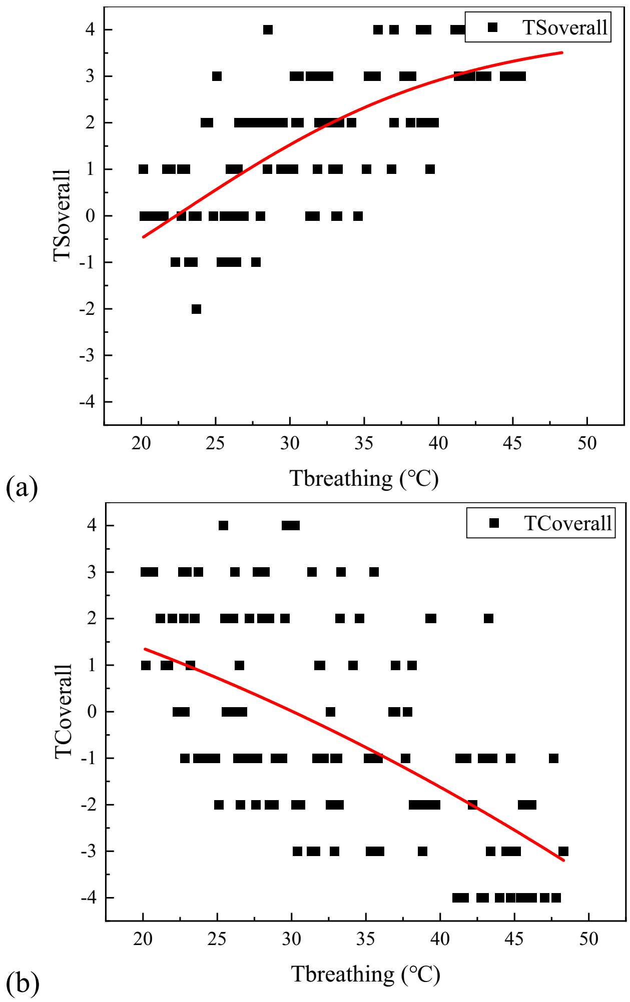

Fig. 11 Correlation between breathing air temperature, overall thermal sensation and overall thermal comfort

Based on these two key factors, a human thermal sensation and thermal comfort evaluation model based on environmental factors and skin temperature was established.

3.6.1 Overall Thermal Sensation

Firstly, a single-factor thermal sensation prediction model was established according to breathing air temperature and chest skin. Then, a complete thermal sensation model was based on multiple linear analyses to comprehensively consider the effect of the temperature of breathing air and chest skin surface on the overall thermal sensation. The constants obtained from the fit are shown in Equation.

$$OTS_{breathingair} = \frac{8}{\left(1 + \exp\left(-0.105 * \left(T_{breathingair} - 22.337\right)\right)\right)} - 4 \quad (4)$$

$$OTS_{chest} = \frac{8}{\left(1 + \exp\left(-0.545 * \left(T_{chest} - 33.203\right)\right)\right)} - 4 \quad (5)$$

$$\text{OTS} = 0.765 * OTS_{breathingair} + 0.365 * OTS_{trunk} - 0.176\left(R^2 = 0.61\right) \quad (6)$$

3.6.2 Overall Thermal Comfort

According to the previous research, ambient and skin temperature choices could not obtain a better thermal comfort model. Based on overall thermal sensation, this study developed a prediction model for overall thermal comfort in car cabins.

$$\text{OTC} = -9.412 + 10.467 * e^{-\frac{(OTS+0.517)^2}{44.92}} \left(R^2 = 0.39\right) \quad (7)$$

3.7 Validation of the In-Vehicle OTS and OTC Prediction Model

Through the above research, we get the human body's prediction model of OTS and OTC in the vehicle cabin. A total of 128 participants participated in the experiment, with data from 98 participants used to derive the equations. And other data from 30 participants were used to test the accuracy of the prediction model. A tenfold cross-validation of the average performance of this modeling method was used. Validation was carried out by comparing the measured OTS value with the predicted OTS value, calculated from derived equations. Figure 14 illustrates the impact of the OTS and OTC prediction models, with the X-axis representing the measured OTS or OTC value, and the Y-axis representing the predicted value. The R^2 values for the OTS and OTC prediction models are relatively high at 0.77 and 0.51, respectively. Despite being randomly selected, we can observe from the figure that overall thermal sensation of the experimental samples is hot; however, overall thermal comfort is not satisfactory.

Table 3 R^2 between overall thermal sensation (OTS) and overall thermal comfort (OTC) and environmental temperature

Environmental factor	Environment	Dashboard	Windshield	Roof	Breathing air	Foot air
R^2 (OTS)	0.31	0.15	0.17	0.36	0.58	0.16
R^2 (OTC)	0.03	0	0.01	0.43	0.34	0.08

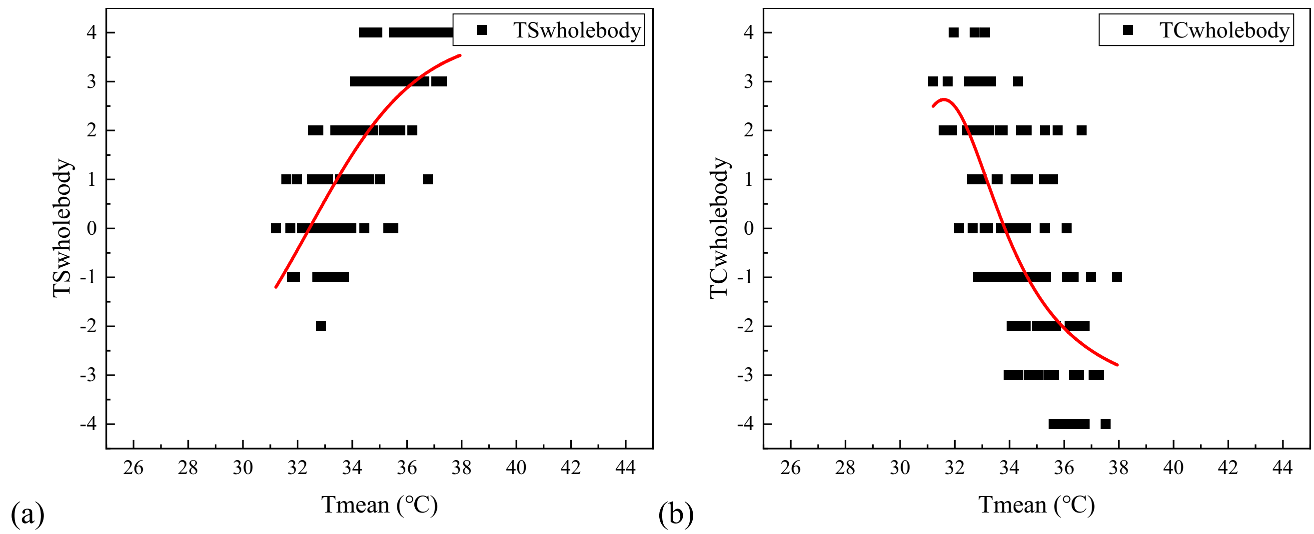

Fig. 12 Correlation between mean skin temperature, overall thermal sensation and overall thermal comfort

Table 4 Regression coefficients and R^2 of overall thermal sensation (OTS) and overall thermal comfort (OTC) in relation to skin temperature

Body part	Head	Chest	Upper arm	Lower arm	hand	Thigh	Calf	Foot	Whole body
R^2 (OTS)	0.46	0.54	0.39	0.41	0.41	0.2	0.43	0.26	0.55
R^2 (OTC)	0.24	0.39	0.24	0.24	0.43	0.33	0.44	0.32	0.51

4 Discussion

The thermal environment in the passenger compartment of an automobile is influenced by the air conditioning system's air supply conditions (temperature, speed, direction), solar radiation, external ambient temperature, and other parameters. The modes of heat transfer between the human body and the environment in the vehicle include heat convection, heat radiation, heat conduction, and evaporative heat transfer. Compared to the heat transfer in a building, the human body in a vehicle exchanges more heat by radiation and conduction due to the large proportion of glass area. Solar radiation enters the cabin either by transmission or absorption; transmitted short-wave radiation is received directly by the occupants, and absorbed solar radiation enhances long-wave radiative heat exchange to the human body by increasing the surface temperature of the cabin. The human body exchanges conductive heat with the seats and steering wheel in contact. The operating air conditioning system generates an inhomogeneous temperature field around the driver and occupant so that the amount of convective heat exchange is different for each part of the body. Due to the directional nature of direct shortwave solar radiation, this radiation can only be received by certain parts of the body. Airflow organization can also be highly heterogeneous and transient due to the restricted space and complex shape of the vehicle interior, all of which contribute to the differences between the indoor environments of automobiles and buildings.

Under uniform or non-uniform thermal conditions, many researchers have established human thermal sensation and thermal comfort models. However, most study is based totally on a controlled laboratory environment. The natural temperature environment in the car's cabin differs greatly from the artificially manufactured non-uniform thermal environment, which makes the prediction model developed under laboratory settings drastically different in the real world. When assessing a person's thermal comfort inside a car, it is more helpful to forecast their overall thermal sensation and overall thermal comfort than their local thermal sensation and local thermal comfort. It is challenging to measure so many parameters during the actual evaluation process when using the previous prediction model to assess the human thermal comfort inside an automobile's cabin because it requires a lot of environmental parameters, skin surface, and core temperature measurements. The measurement of these parameters is not only time-consuming and laborious, but also affects the subject at the physiological and psychological level, which in turn influences the person's subjective evaluation.

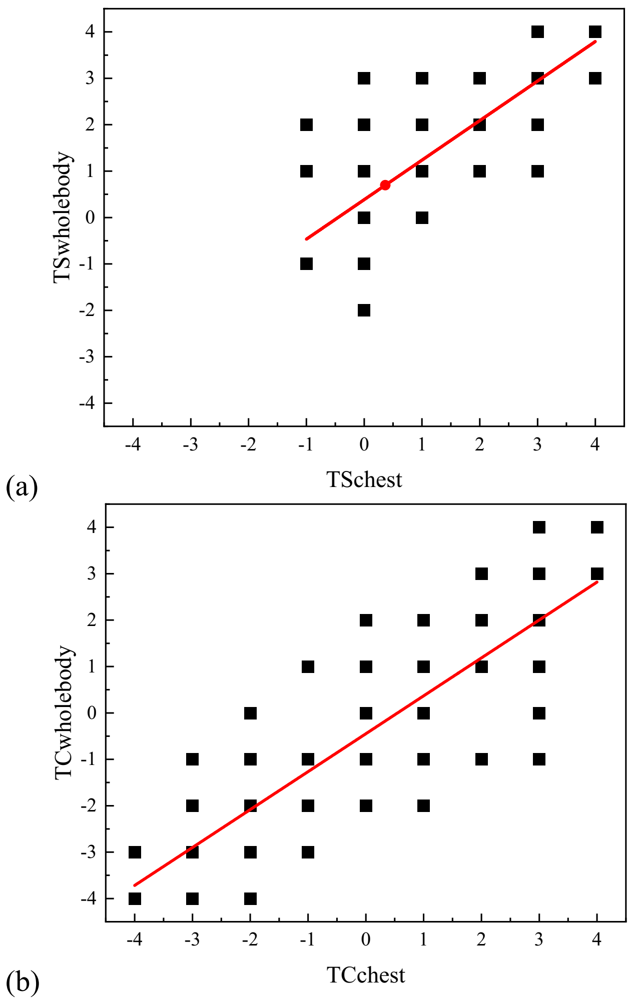

Fig. 13 Relationship between local and overall thermal sensation and thermal comfort. **a** Chest thermal sensation and **b** chest thermal comfort

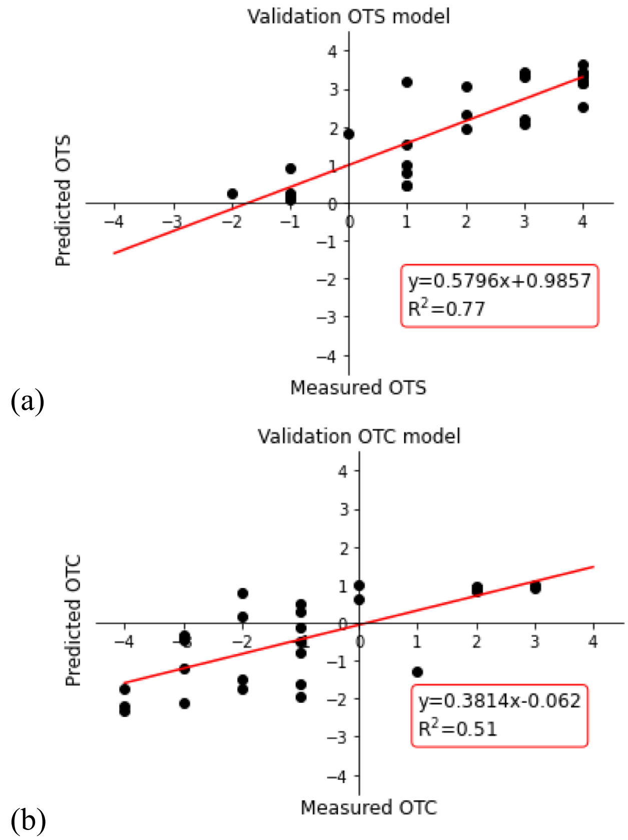

Fig. 14 Validations on developed OTS model and OTC model

In this paper, we tried to discover the quantity that best characterized the overall thermal sensation and comfort in the vehicle cabin. The environmental and human factors used as few variables as possible to fit and derive the prediction model of overall thermal sensation and overall thermal comfort. By a previous study of the human subjective evaluation and environmental laws between the temperature and skin temperature variables, this study selected logic function to the overall thermal sensation associated with breathing air temperature and chest skin temperature and obtained by multiple linear regression based on environment temperature variables and skin temperature prediction model of whole-body thermal sensation. For thermal comfort, we found that the performance of thermal comfort prediction models based on thermal sensation is better than the comfort model based on skin temperature. In this study, the Gaussian function relates thermal comfort to thermal sensation. The overall thermal sensation and thermal comfort prediction models had higher R^2 values of 0.77 and 0.51, respectively. This suggests that the thermal sensation fit has better correlation than thermal comfort. The underlying reason for this is that the differences in thermal comfort are more pronounced in the human body. Furthermore, the mathematical basis for the overall thermal comfort model was not provided in earlier investigations.

Table 5 R^2 of local thermal sensation and thermal comfort in relation to overall thermal sensation and comfort

Body part	Head	Chest	Upper arm	Lower arm	hand	Thigh	Calf	Foot
Slope for thermal sensation	0.89	0.85	0.67	0.64	0.57	0.58	0.67	0.60
R^2 for thermal sensation	0.69	0.72	0.45	0.39	0.36	0.35	0.42	0.32
Slope for thermal comfort	0.94	0.95	0.54	0.55	0.52	0.57	0.53	0.51
R^2 for thermal comfort	0.80	0.77	0.30	0.31	0.30	0.31	0.29	0.29

Through the collection of human subjective evaluation experimental data, it is found that most subjects are in a relatively hot overall thermal sensation state under various working conditions. Due to the lack of data on rather cold and hot sensations, the fitted prediction model of overall thermal sensation and thermal comfort has a deviation. Future experiments under colder conditions can be added to improve the prediction model. In addition, this study is limited to the stationary state of parked vehicles, so it is impossible to study the differences in environmental conditions and passenger thermal comfort under actual driving conditions. Due to the cabin's complex and changeable thermal environment, this study only considers the effect of the environment's temperature and skin surface on the subjective evaluation of the human body. In the future, further analysis can be carried out on factors that significantly influence the cabin's thermal environment, for instance, wind speed and radiation intensity, to establish a more robust and comprehensive model.

5 Conclusion

In this study, the relationship between thermal sensation and comfort, thermal environment in vehicle cabin, the ambient and skin surface temperature was analyzed and prediction models for overall thermal sensation and overall thermal comfort were established by using field experiments to analyze human thermal comfort in the vehicle passenger compartment. Breathing air and chest skin surface temperature were the factors which significantly associated with overall thermal sensation in thermal environment and human factors, respectively. These two factors have a strong correlation with the overall thermal sensation in the vehicle occupant compartment with an R^2 value of 0.61. In contrast, thermal sensation as an input quantity better characterizes thermal comfort compared to skin temperature or thermal environment. However, the correlation between overall thermal sensation and overall thermal comfort is relatively poor, and its R^2 value is 0.39. The results of the tenfold cross-validation show that the prediction model of overall thermal sensation and thermal comfort has good prediction performance, with R^2 values of 0.77 and 0.51, respectively. Since most subjects are in a hot thermal sensation state under the experimental condition, further research is planned to create a cooler thermal environment in the vehicle's cabin and establish a complete prediction model. In addition, an attempt is made to analyze the correlation between other influencing factors besides temperature, such as wind speed, solar radiation intensity, EEG signal and subjective human evaluation, to establish a more robust prediction model for automotive thermal comfort and provide a scientific basis for automotive air conditioning control strategies.

Acknowledgements The author(s) disclosed receipt of the following financial supports for the research, authorship, and/or publication of this article: This work is supported by National Key R&D Program of China (2022YFE0208000), the Fundamental Research Funds for the Central Universities.

Data availability The data that support the findings of this study are available on request from the corresponding author upon reasonable request.

Declarations

Conflict of interest The authors declare that they have no conflict of interest.

References

Alahmer, A., Abdelhamid, M., & Omar, M. (2012). Design for thermal sensation and comfort states in vehicles cabins. *Applied Thermal Engineering, 36*, 126–140.

Croitoru, C., Nastase, I., Bode, F., Meslem, A., & Dogeanu, A. (2015). Thermal comfort models for indoor spaces and vehicles-Current capabilities and future perspectives. *Renewable & Sustainable Energy Reviews, 44*, 304–318.

Danca, P., Vartires, A., & Dogeanu, A. (2015). *An overview of current methods for thermal comfort assessment in vehicle cabin*. Romania: Bucharest.

Fanger, P. O. (1967). Calculation of thermal comfort, introduction of a basic comfort equation. *ASHRAE Transactions, 73*(2), 1–20.

Hardy, J. D. (1938). The technic of measuring radiation and convection. *Burnal of Nutrition*. https://doi.org/10.1093/jn/15.5.461

Hepokoski, M., Curran, A., Viola, T., Lindedal, N., Hansson, R. and Gullman, S. (2018). Evaluating a Vehicle Climate Control System with a Passive Sensor Manikin coupled with a Thermal Comfort Model. 1.

Hepokoski, M., Viola, T., Juszkiewicz, J., Tetzloff, L. and Blough, J. (2021). A Novel Methodology to Characterize the Thermal Behavior of Automotive Seats.

Hu, Y. X., Zhao, L. P., Xu, X., Wu, G. M., & Yang, Z. G. (2024). Experimental Study on Thermal Environment and Thermal Comfort of Passenger Compartment in Winter with Personal Comfort System. *Energies, 17*, 9.

Kaynakli, O., Pulat, E., & Kilic, M. (2005). Thermal comfort during heating and cooling periods in an automobile. *Heat and Mass Transfer, 41*(5), 449–458.

Kaynakli, O., & Kilic, M. (2005). An investigation of thermal comfort inside an automobile during the heating period. *Applied Ergonomics, 36*(3), 301–312.

Kilic, M., & Kaynakli, O. (2011). An experimental investigation on interior thermal conditions and human body temperature during cooling period in automobile. *Heat and Mass Transfer, 47*(4), 407–418.

Kilic, M., & Akyol, S. M. (2012). Experimental investigation of thermal comfort and air quality in an automobile cabin during the cooling period. *Heat and Mass Transfer, 48*(8), 1375–1384.

Kim, Y., Lee, M., Shin, Y., & Cho, H. (2023). Investigation of changes in Driver?s biosignals and thermal comfort according to the heating method in winter. *Case Studies in Thermal Engineering*. https://doi.org/10.1016/j.csite.2023.102749

Lee, D., & Lee, H. (2020). Impact of Focus- and Diffuse-Type Air Vents on Cabin Thermal Comfort. *International Journal of Automotive Technology, 21*(5), 1315–1322.

Mao, Y. Y., Wang, J., & Li, J. M. (2018). Experimental and numerical study of air flow and temperature variations in an electric vehicle cabin during cooling and heating. *Applied Thermal Engineering, 137*, 356–367.

Nastase, I., Danca, P., Bode, F., Croitoru, C., Fechete, L., Sandu, M., & Cosoiu, C. I. (2022). A regard on the thermal comfort theories from the standpoint of electric vehicle design - review and perspectives. *Energy Reports, 8*, 10501–10517.

Neacsu, C., Tabacu, I., Ivanescu, M., Vieru, I., & Iop. (2017). *The evaluation of the overall thermal comfort inside a vehicle*. Romania: Pitesti.

Oi, H., Yanagi, K., Tabata, K., & Tochihara, Y. (2011). Effects of heated seat and foot heater on thermal comfort and heater energy consumption in vehicle. *Ergonomics, 54*(8), 690–699.

Oi, H., Tabata, K., Naka, Y., Takeda, A., & Tochihara, Y. (2012). Effects of heated seats in vehicles on thermal comfort during the initial warm-up period. *Applied Ergonomics, 43*(2), 360–367.

Wyon, D. P., Larsson, S., Forsgren, B. and Lundgren, I. (1989). Standard Procedures for Assessing Vehicle Climate with a Thermal Manikin.

Xu, X., Zhao, L., and Yang, Z., "Field Experimental Investigation on Human Thermal Comfort in Vehicle Cabin," SAE Technical Paper 2022–01–0195, 2022, https://doi.org/10.4271/2022-01-0195.

Yun, S., Chun, C., Kwak, J., Park, J. S., Kwon, C., Kim, S., & Seo, S. (2021). Prediction of thermal comfort of female passengers in a vehicle based on an outdoor experiment. *Energy and Buildings*. https://doi.org/10.1016/j.enbuild.2021.111161

Zhang, H., Arens, E., Huizenga, C. and Han, T. (2009). Thermal sensation and comfort models for non-uniform and transient environments: Part I: local sensation of individual body parts. Building and Environment.

Zhang, H., Arens, E., Huizenga, C., & Han, T. (2010a). Thermal sensation and comfort models for non-uniform and transient environments, part II: Local comfort of individual body parts. *Building and Environment, 45*(2), 389–398.

Zhang, H., Arens, E., Huizenga, C., & Han, T. (2010b). Thermal sensation and comfort models for non-uniform and transient environments, part III: Whole-body sensation and comfort. *Building and Environment, 45*(2), 399–410.

Zhao, Y., Zhang, H., Arens, E. A., & Zhao, Q. C. (2014). Thermal sensation and comfort models for non-uniform and transient environments, part IV: Adaptive neutral setpoints and smoothed whole-body sensation model. *Building and Environment, 72*, 300–308.

Zhou, X., Lai, D., & Chen, Q. (2019). Experimental investigation of thermal comfort in a passenger car under driving conditions. *Building and Environment, 149*, 109–119.